

Photodissociation Dynamics of Cyanamide at 193 nm: The CN Radical Production Channel

Ji Hye Lee, Tae Yeon Kang, Hyonseok Hwang, Chan Ho Kwon, and Hong Lae Kim*

Department of Chemistry, College of Natural Sciences, Institute for Molecular Science and Fusion Technology, Kangwon National University, Chunchun 200-701, Korea. *E-mail: hlkim@kangwon.ac.kr
Received June 4, 2008

Photodissociation dynamics of cyanamide (NH_2CN) at 193 nm has been investigated by measuring rotationally resolved laser induced fluorescence spectra of CN fragments, from which rotational population distributions of CN as well as translational energy releases in the products were obtained. From quantum chemical molecular orbital calculations, a mixture of the $n \rightarrow \pi^*$ and the transition to a state of the ionic character was found to be responsible for the absorption whereas the $n \rightarrow \sigma^*$ transition results in the absorption at 212 nm where the dynamics of dissociation was previously studied. The observed energy partitioning was well represented by statistical prior calculations, from which it was concluded that the dissociation takes place on the ground electronic surface after rapid internal conversion.

Key Words : Cyanamide, Internal conversion, Laser induced fluorescence, Photochemistry, Statistical energy partitioning

Introduction

Molecular structures of cyanamide (NH_2CN) have been extensively studied by Microwave and high resolution Fourier Transform Infrared spectroscopy and by theoretical calculations, from which the pyramidal structure about the amino nitrogen was determined.¹⁻⁶ In the gas phase, cyanamide is in equilibrium with carbodiimide that is a condensing agent able to induce the formation of peptides from amino acids.⁷ The isomerization of cyanamide into carbodiimide was observed either when cyanamide was condensed at low temperature (80 K) on an amorphous water ice surface as catalysis or by VUV irradiation at low temperature (10 K) in Ar or water matrix, and solid films.^{8,9} Photochemistry and photophysics of cyanamide in the gas phase is of a considerable interest because it is a prebiotic molecule. However, any UV absorption spectrum and hence studies of cyanamide in the excited electronic states have not yet been reported but one. Photodissociation dynamics of cyanamide at 212 nm was reported, in which dissociation on the ground electronic state was suggested from the observed energy partitioning among the products.¹⁰

In RCN molecules, a simple bond fission producing CN radicals was observed upon UV irradiation. The lowest electronic transition in UV is mainly assigned as the $n \rightarrow \pi^*$ or the $\pi \rightarrow \pi^*$ electronic transition depending upon the molecules studied, from which the dissociation takes places either on the excited state *via* predissociation or on the ground state *via* internal conversion. In CH_3CN , considerable rotational excitation of the CN fragments was observed implying a bent geometry in the repulsive excited state.¹¹ On the other hand, in acrylonitrile and isomers of 2-butene-nitrile, a statistical energy partitioning among products was observed, which implies slow dissociation on the ground state after the internal conversion.¹²⁻¹⁵ However, in alkyl

amines, the electronic transition in UV excites the molecules in the Rydberg state and the predissociation takes place *via* excessive potential couplings.¹⁶ Since the dissociation dynamics should be governed by the nature of the electronic transition and by the shape of the potential energy surfaces leading to the individual product channels, physical processes in the electronically excited states can be investigated by studying the photodissociation dynamics as well as the UV absorption spectra.

In this report, the UV absorption spectrum of cyanamide was measured and analyzed in relation to the results of quantum chemical molecular orbital calculations. In addition, a rotationally resolved laser induced fluorescence (LIF) spectrum of CN produced from the photodissociation of cyanamide at 193 nm was measured, from which energy partitioning among the products was obtained. The detailed dissociation dynamics was discussed from the absorption spectrum and the observed energy partitioning.

Experiments

The experiments were performed in a flow cell with conventional pump-probe geometry. The cell was evacuated at a pressure of 10^{-3} Torr with a mechanical pump. The solid sample of cyanamide was heated and the vapor of liquid (mp: 45 °C) at 60 °C was slowly flowed through the cell at a pressure of about 80 mTorr, which was controlled by needle valves. The stated purity of 99% of solid cyanamide was purchased from Aldrich and used without further purification.

The photolysis light at 193 nm was an output of an ArF excimer laser (PSX-100, MPB), which was unpolarized. The photolysis light beam was shaped as a circle (~4 mm dia. and ~8 mJ/cm²) with baffles that are placed inside arms attached to the cell. The baffles also minimized the scattered

radiation into the detector. The probe light to measure laser induced fluorescence spectra of CN at 389–382 nm employing B-X transition was an output of a dye laser (HD-500, Lumonics) pumped by the third harmonic of an Nd:YAG laser (YM-800, Lumonics). The horizontally polarized dye laser output was collinearly counterpropagated to the photolysis laser beam. The power of the probe light was kept as low as possible to avoid saturation in the spectra, which was typically about $30 \mu\text{J}/\text{pulse}$ ($\sim 4 \text{ mm}$ dia.). The LIF signal vs. photolysis laser power showed linear dependence up to $20 \text{ mJ}/\text{cm}^2$, which ensured one-photon dissociation at the typical power used. The fluorescence signal was detected with a photomultiplier tube (1P28A, Hamamatsu) perpendicularly mounted relative to the laser beams through cut-off filters to reduce scattered radiation of the photolysis light. The measured signal was fed to a digital sampling oscilloscope and integrated fluorescence signals were recorded. The delay between the pump and probe, typically about 100 ns was controlled with a digital pulse and delay generator. The sample pressure of 80 mTorr and the 100 ns delay time should provide a nascent product energy distribution. The measured fluorescence spectra were corrected with variation of the pump and probe laser powers and stored in a PC.

The laser line profile was measured from the rotational line profile of CN after translational relaxation by collisions. A Doppler line profile of one of the low N rotational transitions was measured at 2 μsec pump-probe delay and 5 Torr Ar as a colliding gas, from which the laser line profile was measured after deconvolution of a Gaussian Doppler profile of CN at 300 K assuming complete relaxation. At this time delay and even higher pressure of Ar, no change in the profile and rotational relaxation to 300 K was observed. The estimated FWHM of the Lorentzian laser line profile was 0.27 cm^{-1} .

Results and Discussion

A. LIF spectra and rotational energies of CN. The LIF spectra of CN ($X^2\Sigma$, v'' , N) produced from photodissociation of cyanamide at 193 nm employing the $^2\Sigma \leftarrow ^2\Sigma$, B \leftarrow X electronic transition are presented in Figure 1. In the spectra, the P-branch bandheads of the 0-0 and 1-1 vibrational transitions clearly appear and the assignments for the R-branch rotational transitions are given on top of the spectra.¹⁷ The LIF signal in the region of 2-2 vibrational transition was negligibly small compared to the noise in the spectra, from which no vibrational population in $v'' = 2$ is assumed. The individual transitions would result from excitations of pairs of the spin doublets corresponding to $J = N \pm 1/2$ in these spectra according to the Hund case (b) electronic and rotational angular momentum couplings. The rotational population distributions were obtained from integrated intensities of the peaks corrected by appropriate line strength factors that are proportional to the square of the electronic transition moment, the Franck-Condon factors, and the Hönl-London factors, $2(N+1)$ in this case. The average

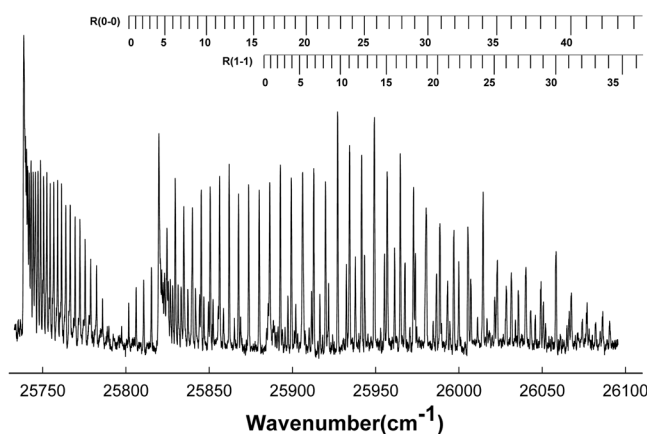


Figure 1. Laser induced fluorescence spectra of CN produced from photodissociation of cyanamide at 193 nm employing the B-X electronic transition.

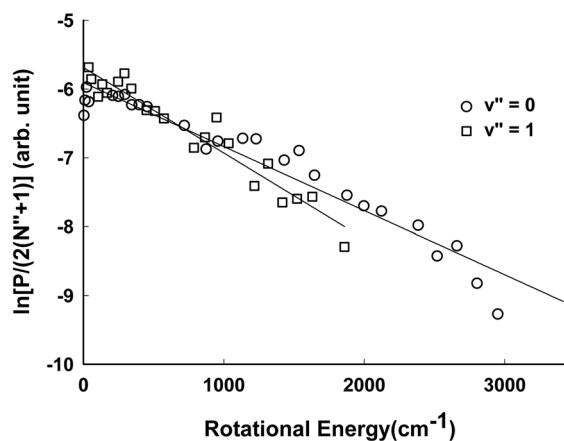


Figure 2. Boltzmann plots of rotational energy distribution of CN obtained from Figure 1.

rotational energies of CN were then obtained from linear slopes of the Boltzmann plots, which were $1,080 \pm 40$ and $800 \pm 30 \text{ cm}^{-1}$ for $v'' = 0$ and $v'' = 1$, respectively (Figure 2).

B. Translational energy releases. In order to measure translational energies of the fragments, the Doppler profiles of the individual rotational transitions in the spectra were analyzed. In Figure 3, the Doppler broadened spectrum for $N = 4$ in the R-branch rotational transitions is presented. The rotational transitions from the two spin doublet states were nearly overlapped at low N and almost resolved at high N under the given resolution of our laser. Since the separation of the two transitions at $N = 4$ is 0.06 cm^{-1} , the measured profile was estimated as the sum of the two transitions, which was fitted well with two Gaussian profiles implying isotropic velocity distribution for CN. One might argue that the Doppler profiles should have distinct shape for each rotational branch transition probed even for the case of isotropic velocity distribution of the photofragments due to so-called the v-j vector correlations developed at the moment of impulse of the dissociation.¹⁸ However, since the P and R-branch rotational transitions could only be probed for the B-X electronic transition of CN according to the

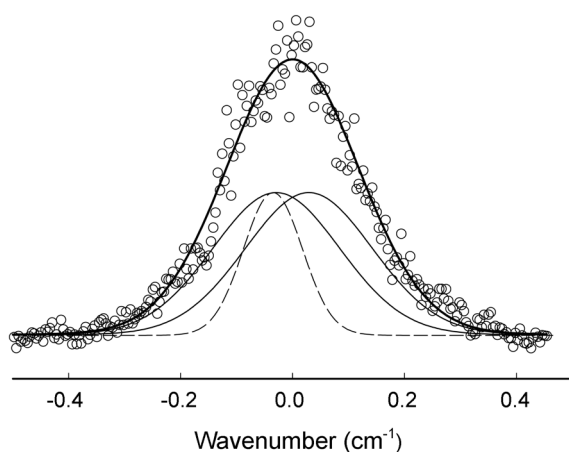


Figure 3. Doppler profiles of the $R_{0-0}(4)$ rotational transition of CN. The dashed line is the laser line profile and the solid lines are the actual Doppler profiles after deconvolution of the laser line profile.

selection rules at the present study, no Q-branch transitions could be measured for comparison of the profiles. Then, the actual Gaussian Doppler profiles were extracted by deconvolution of the measured laser line profile. The average translational energy of CN at $v'' = 0$ and $N = 4$ was measured from the second moment of the profiles obtained from the best fit and then the center of mass translational energy release in the products was calculated to be $4,440 \pm 300 \text{ cm}^{-1}$. The observed energy partitioning is summarized in Table 1 together with those from model calculations discussed below.

C. Excited states and dissociation mechanism. The UV spectrum of cyanamide taken in water as a solvent because the sample is solid at ambient temperature, showed continuously increasing absorption starting from 240 nm with a shoulder near 220 nm. In order to characterize the nature of the electronic transition, quantum chemical molecular orbital calculations were performed. The time dependent density functional theory (TD-DFT) calculations were carried out at the B3LYP/6-311++G** level employing the Gaussian 03 package of programs.¹⁹ At the vertical transition energy of 6.4045 eV (193.59 nm), the electronic transition turns out to have the mixed character, $11 \rightarrow 13$ and $11 \rightarrow 14$, the $n \rightarrow \pi^*$ and the transition to a state of the ionic character with $\text{H}_2\text{N}^+=\text{C}=\text{N}^-$ configuration, respectively, which implies indirect dissociation of the N-C bond *via* potential couplings.

In order to figure out dissociation mechanism, spin correlation arguments are extremely helpful. The reaction energy was obtained by the enthalpies of formation of NH_2 and CN

Table 1. Energy partitioning among products (in cm^{-1}) produced from photodissociation of cyanamide at 193 nm

	$\langle E_t(\text{CN}) \rangle$		$\langle E_r \rangle$	
	$v'' = 0$	$v'' = 1$	$v'' = 0$	$v'' = 1$
Experiment	$1,080 \pm 30$	800 ± 30	$4,440 \pm 300$	$4,070 \pm 450$
Prior	1,284	880	4,762	4,035
Impulsive	2,423	1,966	7,486	6,072

from literatures and the enthalpy of formation of NH_2CN calculated by *ab initio* calculations at the MP2/6-311++G** level with G2 corrections using the Gaussian 03 package of programs because of no thermochemical data for NH_2CN .²⁰ Then, the calculated available energy for energy partitioning in the products, the photon energy at 193 nm minus the dissociation energy, was calculated to be $10,813 \text{ cm}^{-1}$. The energies of NH_2 (A^2A_1) and CN ($A^2\Pi$) above the origin on the ground electronic state are $10,250$ and $9,242 \text{ cm}^{-1}$, respectively.^{21,22} Judging from the measured translational energies of the products and the available energy, both fragments should be in their ground doublet states. The two doublet product states must be correlated to three triplet and a singlet parent molecular states. Since the excited singlet parent state should be correlated to either one of the product being in the excited electronic state, the two doublet product states must be correlated to either the ground singlet or the triplet parent state.

Mechanism of photodissociation of molecules could mainly be categorized as three: (1) direct dissociation from a repulsive excited electronic state, (2) predissociation resulting from couplings between excited states, and (3) dissociation on the ground state after internal conversion. In each case, the energy partitioning among degrees of freedom of the products, internal and translational, should be distinctive although it is complicated according to the manner of potential couplings in the case (2). However, simple models can be applied to predict the energy partitioning for the case (1) and (3) such as an impulsive model and a statistical model for the case (1) and (3), respectively. When the dissociation takes place on the triplet surface, it is important to figure out the shape of the potential energy surface along the reaction coordinate. The DFT calculations at the B3LYP/6-311++G** level were performed and there appears no barrier along the reaction coordinate as a result implying dissociation from the repulsive part of the surface as predicted by Zhang and coworkers.²³ In this case, the impulsive model to predict the rotational and translational energies of the products can be applied.^{24,25} Upon the electronic transition, the impulsive model assumes an abrupt turn-on of the repulsive force between atoms of the breaking bond, which results in large translational energy release in the products and then the internal energy distribution of the polyatomic products is developed afterwards. Invoking linear and angular momentum conservations, the average translational and rotational energy of CN was calculated with bent geometry ($\angle \text{NCN} = 121.4^\circ$) obtained by the same density functional theory calculations at the B3LYP/6-311++G** level. The calculated center of mass translational energy release in the products and the rotational energy of CN are $7,486$ and $2,423 \text{ cm}^{-1}$, respectively, which are significantly different from the measured values.

If the dissociation takes place on the ground singlet surface, the energy partitioning can be obtained using the prior model assuming slow dissociation on the vibrationally hot ground electronic state after internal conversion.^{26,27} In this case, the available energy should be distributed among

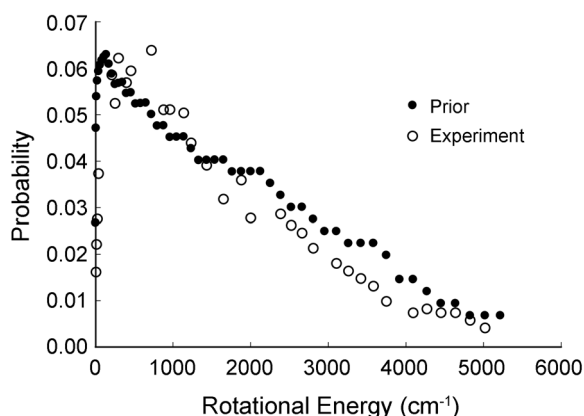


Figure 4. Rotational population distribution of CN at $v''=0$ obtained from the experiment (open circles) and the statistical prior calculations (closed circles).

all product degrees of freedom with equal probability. Thus, the population of the individual rotational state of CN is proportional to the number of accessible quantum states in NH_2 at the energy $E = E_{av} - E_{CN}(v, J)$. The number of vibrational states was directly counted with fundamental vibrational frequencies obtained from the literature.²⁸ The calculated rotational distribution fits well to the observed distribution with minor deviation (Figure 4) but the calculated average rotational energy of $1,284 \text{ cm}^{-1}$ agrees very well to the measured. Similarly, the predicted average translational energy release from the same prior calculation is $4,762 \text{ cm}^{-1}$, which again agrees well with the experiment. The minor deviation of the calculated rotational distribution from the observed should originate from incomplete randomization of the internal energy due to smallness of the molecular size and hence sparse vibrational states. The intramolecular vibrational energy randomization has casually been observed in large polyatomic molecules such as photodissociation of allyl cyanide, where the measured rotational distribution of CN perfectly fits to that from the prior calculations.¹⁴

Conclusions

The photodissociation of NH_2CN upon electronic absorption at 193 nm takes place on the ground electronic state after the internal conversion resulting in statistical energy partitioning among the products.

Acknowledgments. This work was financially supported by the Korea Science and Engineering Foundation.

References

- Vincent, M. V.; Dykstra, C. E. *J. Chem. Phys.* **1980**, *73*, 3838-3842.
- Daoudi, A.; Pouchan, C.; Sauvaire, H. *Chem. Phys. Lett.* **1982**, *91*, 477-483.
- Ichikawa, K.; Hamada, Y.; Sugawara, Y.; Tsuboi, M.; Kato, S.; Morokuma, K. *Chem. Phys.* **1982**, *72*, 301-312.
- Brown, R. D.; Godfrey, P. D.; Kleiboemer, B. *J. Mol. Spectrosc.* **1985**, *114*, 257-273.
- Birk, M.; Winnewisser, M. *Chem. Phys. Lett.* **1986**, *123*, 382-385.
- Birk, M.; Winnewisser, M. *J. Mol. Spectrosc.* **1993**, *159*, 69-78.
- Jabs, W.; Belov, M. S. P.; Lewen, F.; Maiwald, F.; Winnewisser, G. *Mol. Phys.* **1999**, *97*, 213-238.
- Tordini, F.; Bencini, A.; Bruschi, M.; Gioia, L. D.; Zampella, G.; Fantucci, P. *J. Phys. Chem. A* **2003**, *107*, 1188-1196.
- Duvernay, F.; Chiavassa, T.; Borget, F.; Aycard, J. P. *J. Phys. Chem. A* **2005**, *109*, 603-608.
- Kwon, C. H.; Lee, J. H.; Kim, H. L. *Bull. Korean Chem. Soc.* **2007**, *28*, 1485.
- Eng, R.; Filseth, S. V.; Carrington, T.; Dugan, H.; Sadowski, C. M. *Chem. Phys. Lett.* **1988**, *146*, 96-100.
- North, S. W.; Hall, G. E. *Chem. Phys. Lett.* **1996**, *263*, 148-153.
- Li, R.; D-Kovacs, A.; North, S. W. *Chem. Phys.* **2000**, *254*, 309-317.
- Oh, C. Y.; Shin, S. K.; Kim, H. L.; Park, C. R. *Chem. Phys. Lett.* **2001**, *342*, 27-30.
- Oh, C. Y.; Shin, S. K.; Kim, H. L.; Park, C. R. *J. Phys. Chem. A* **2003**, *107*, 4333-4338.
- Baek, S. J.; Choi, K. W.; Choi, Y. S.; Kim, S. K. *J. Chem. Phys.* **2002**, *117*, 10057-10060.
- Prasad, C. V. V.; Bernath, P. F.; Frum, C.; Engelman, Jr., R. *J. Mol. Spectrosc.* **1992**, *151*, 459-473.
- North, S. W.; Hall, G. E. *J. Chem. Phys.* **1996**, *104*, 1864-1874.
- Gaussian 03*; Gaussian Inc.: Pittsburgh, PA, 2003.
- Atkinson, R.; Baulch, D. L.; Cox, R. A.; Hampson, Jr., R. F.; Kerr, J. A.; Rossi, M. J.; Troe, J. *J. Phys. Chem. Ref. Data* **1999**, *28*, 391.
- Herzberg, G. *Molecular Spectra and Molecular Structure III. Electronic Spectra and Electronic Structure of Polyatomic Molecules*; Van Nostrand Reinhold: New York, 1966; p 584.
- Herzberg, G. *Molecular Spectra and Molecular Structure I. Spectra of Diatomic Molecules*; Van Nostrand Reinhold: New York, 1950; p 520.
- Du, B.; Zhang, W. *Int. J. Quantum Chem.* **2006**, *106*, 1827-1843.
- Busch, G. E.; Wilson, K. R. *J. Chem. Phys.* **1972**, *56*, 3626-3638.
- Tuck, A. F. *J. Chem. Soc. Faraday Trans. II* **1977**, *73*, 689-708.
- Zamir, E.; Levin, R. D. *Chem. Phys.* **1980**, *52*, 253-268.
- Levin, R. D.; Bernstein, R. B. *Molecular Reaction Dynamics and Chemical Reactivity*; Oxford Univ. Press: New York, 1987; pp 274-276.
- Jacox, M. E. *J. Phys. Chem. Ref. Data* **1998**, *27*, 133.